

# Moire measurements using a panoramic annular lens

by

John A. Gilbert  
Department of Mechanical Engineering  
University of Alabama in Huntsville  
Huntsville, Alabama 35899

Donald R. Matthys  
Physics Department  
Marquette University  
Milwaukee, Wisconsin 53233

David L. Lehner  
Department of Mechanical Engineering  
University of Alabama in Huntsville  
Huntsville, Alabama 35899

## ABSTRACT

This paper demonstrates that a panoramic annular lens (PAL) can be used to record moire fringes corresponding to the displacement of a grating of constant pitch fixed to a cavity wall. Definitions and parameters used to describe the imaging characteristics of the PAL are combined with the mapping function of the lens to develop analytical relationships sufficient to predict moire fringe loci. Experimental results verify these analytical arguments. The paper also includes discussions of the panoramic annular lens, radial metrology, and potential applications of the panoramic moire method.

## 1. INTRODUCTION

Moire is one of the most refined, precise and simple means of measuring surface displacements.<sup>1</sup> A variety of moire techniques have been developed to measure different displacement components but most of these techniques have been applied on the outer surfaces of structural components. Recently, however, the development of the panoramic annular lens (PAL)<sup>2</sup> has made it possible not only to obtain a wide field of view within a cavity, but to make visual inspections and optical measurements on remote surfaces using a process called radial metrology.<sup>3,4</sup> Some of these techniques are being used for nondestructive evaluation of aerospace components,<sup>5</sup> while others are being targeted for unique applications including the panoramic imaging of tethered systems in space.<sup>6</sup> The present paper describes yet another technique for radial metrology called panoramic moire and demonstrates the first quantitative evaluation of a moire fringe pattern recorded through a PAL system.

## 2. THE PANORAMIC ANNULAR LENS

The panoramic annular lens consists of a single piece of glass with spherical surfaces that produces a flat annular image of the entire 360 degree surround of the optical axis of the lens. As illustrated in Figure 1, light is reflected and refracted within the lens to form a virtual image. This image must be transferred to an image capturing device using a collector lens. This is illustrated in Figure 2 which shows the schematic of a typical PAL imaging system. The system includes a 50 mm diameter PAL mounted with an f/1.4, 25 mm focal length collector lens. The field of view extends from about 12 to 47 degrees above the lens; a "C" mount is included so that the system can be attached to a standard video camera. The most outstanding attributes of the PAL are that there are no moving parts, the area surrounding the lens can be viewed simultaneously, and the depth of focus extends from its surface to infinity. These attributes make it possible to measure displacements within cavities using the technique of radial metrology.

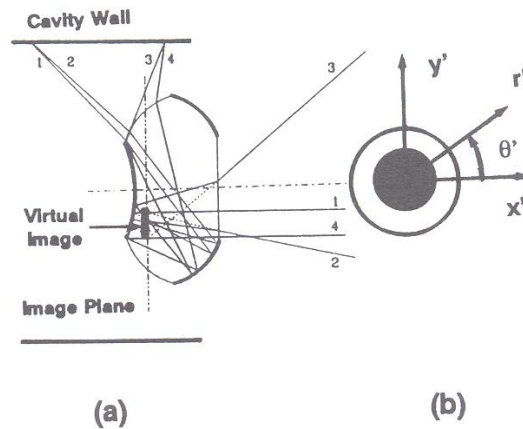
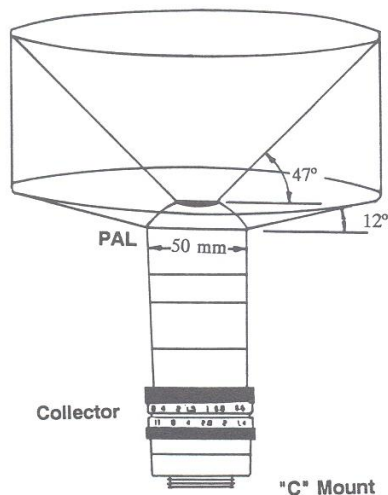
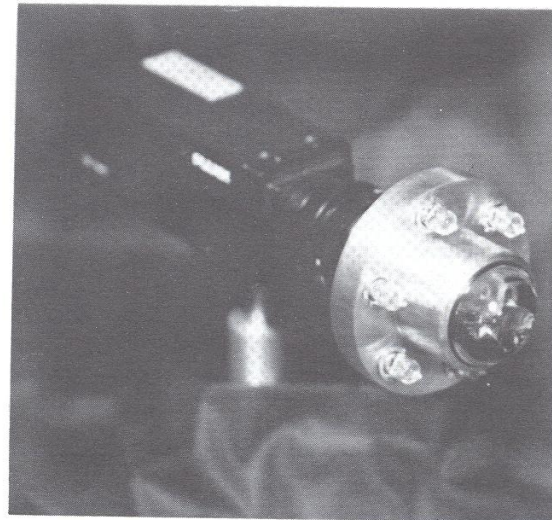


Figure 1. (a) Ray diagram for a PAL; (b) Coordinate systems  $(x',y')$  and  $(r',\theta')$  have been superimposed on the annular image to help define the image plane.



**Figure 2.** The field of view for a 50 mm diameter PAL imaging system. Figure provided courtesy of Optechnology, Inc., Huntsville, AL.



**Figure 3.** A ring of lights may be used to surround a PAL system for illumination within cavities.

### 3. RADIAL METROLOGY

Radial metrology combines standard optical techniques with a panoramic lens and a computer system for cavity inspection and measurement. Figure 3, for example, shows one of the prototypes developed for panoramic moiré and illustrates how the system depicted in Figure 2 can be adapted for cavity inspection. In Figure 3, the PAL is surrounded by a ring containing a number of discrete light sources for illumination; the prototype is mounted on a standard CCD camera (Pulnix TM-845) having a resolution of 512 x 512 pixels. The hardware platform selected for acquiring and storing images was an 80386 microprocessor running on a standard AT bus under the MS-DOS operating system (Dell System 310). Images were acquired by a standard commercial frame grabber and processor (Matrox MVP-AT) and stored in the Dell 310 computer.

### 4. PANORAMIC MOIRÉ

This paper demonstrates that a PAL can be used to record moiré fringes corresponding to the displacement of a grating of constant pitch fixed to a cavity wall. Analytical arguments, which take into account the unique mapping of the PAL system, are verified experimentally; thereby establishing the creditability for this new technique called panoramic moiré.

Panoramic moiré is being developed for NASA's Marshall Space Flight Center and is expected to provide a new inspection capability for the Space Shuttle Main Engine program. It may be used to verify the condition of space hardware after manufacturing, to perform inservice inspections following ground test engine firings, and to predict potential failure sites during refurbishment between shuttle flights. The ability for identifying and locating internal flaws, measuring the depth of surface cracks, comparing design contours to actual part contours, performing automated dimensional inspections, and establishing the relationship of the details in a complex assembly will be of tremendous importance to the space program.

For example, panoramic moiré could be used to accurately measure geometrical changes which may occur within a rocket engine's nozzle and combustion chamber. The geometries of these components are critical for optimum performance of the engine. If the geometry of the combustion chamber is not properly maintained, acoustic instabilities may occur as propellants are converted into high-pressure, high-temperature gases. Should acoustic



resonance occur, the combustion process could be inhibited or severe damage to hardware could result. The nozzle is shaped to control the expansion of the exhausting gases so that the thermal energy of combustion is efficiently converted into kinetic energy required to produce thrust. Subtle changes in nozzle geometry may have a detrimental effect on overall engine performance.

Panoramic moiré may also be valuable for in-space measurement of space-assembled structures, deployed structures, and manned systems. A typical monitoring sequence may include characterization of defects or alignment of subsystems appropriate with mission requirements. The parameters to be monitored may include dimensional precision and the stiffness or strength of truss members, joints, beams and structural supports. Inspections may be performed to look for deformation, externally-induced damage occurring as a result of impact from space debris or meteorites, or internally-induced damage such as fatigue or creep resulting from changes in frequency, stiffness, or temperature.

Other applications may include detection or characterization of flaws in composite materials, detection of inhomogeneities in metal castings, determination or verification of internal geometry, assessment of internal configuration and failure analysis support, detection of materials anomalies, determination of structural integrity, and development of acceptance criteria for critical components.

### 5. PAL IMAGING CHARACTERISTICS

The field of view of a PAL may be defined in terms of its upper and lower axial field angles typically measured from the optical axis of the lens. These angles are denoted as  $\alpha_u$  and  $\alpha_l$ , respectively; for the PAL system shown in Figure 2,  $\alpha_u = 43^\circ$  and  $\alpha_l = 78^\circ$ . Obviously, it would be desirable to make  $\alpha_u$  small and  $\alpha_l$  large, so as to maximize the viewed surface, but restrictions are imposed on the values of these parameters by the limited range of values of the index of refraction that can be obtained in commercially available glasses. The width of the annular image corresponds to the size of the acceptance angle ( $\alpha_l - \alpha_u$ ), and each concentric ring in the image plane is the locus of points recorded at a fixed angle to the optical axis.

As illustrated in Figure 4, the imaging characteristics of the PAL may be described with respect to a circular ring, called the offset, defined by the loci of the points of intersection of rays corresponding to the upper and lower axial field angles. The ring lies in the offset plane and is defined relative to the front of the lens; the axial offset,  $a_o$ , is the distance measured from the offset plane to the front of the lens while the radial offset,  $r_o$ , is measured perpendicular to the optical axis and equals the radius of the ring. The axial offset is defined as positive when the offset plane lies behind the front surface of the PAL (toward the imaging block), while the radial offset is positive when each point forming the ring lies on the opposite side of the optical axis from the surface being viewed. For the lens shown in Figure 2,  $a_o = 0.5$  cm (0.251") and  $r_o = -0.335$  cm (-0.132"). An offset axis, parallel to the optical axis of the lens, can be defined for each point in the offset plane; the loci of offset axes forms a circular cylinder centered around the optical axis of the PAL. Object space is described by the cartesian ( $x, y, z$ ) and cylindrical ( $r, \theta, z$ ) axes shown superimposed on Figure 4.

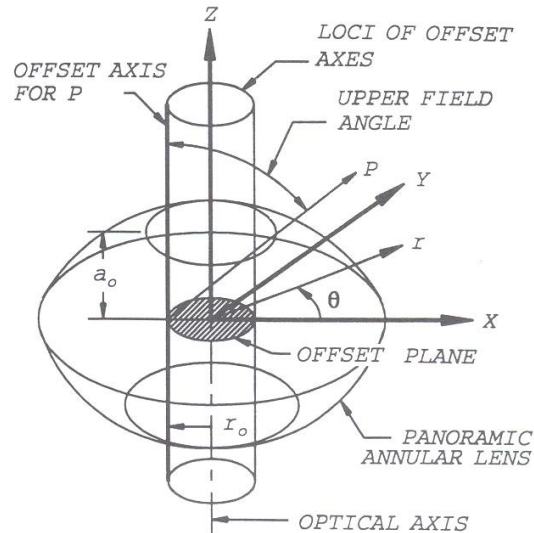
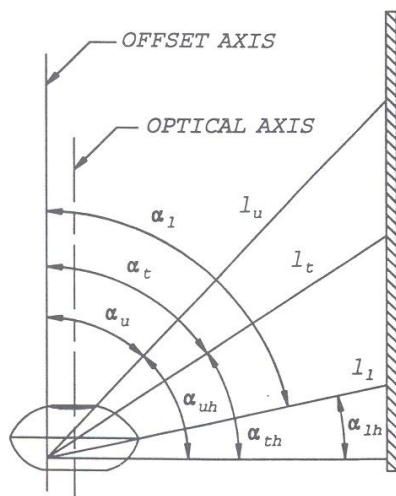
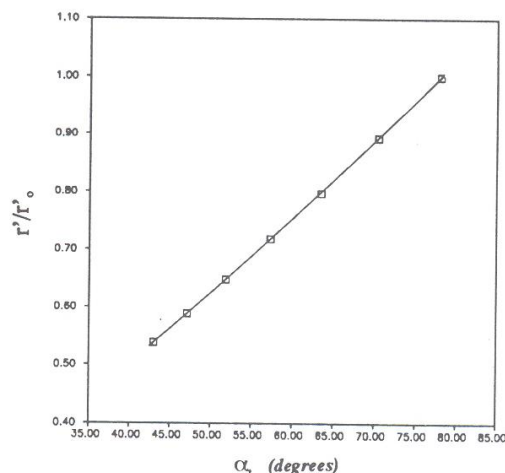


Figure 4. The imaging characteristics of a PAL may be described in terms of its offset.

In Figure 5, a PAL is shown unmounted and placed inside a cavity in the same orientation as the lens depicted in Figures 2 and 4. In this case, the upper and lower axial field angles are measured relative to the offset axis. The angle  $\alpha_l$  is the axial field angle



**Figure 5.** Axial field angles are measured relative to the offset axis; whereas, field angles are measured from the horizon.



**Figure 6.** The mapping function for a 50 mm diameter PAL.

corresponding to a target point located on a cavity wall. The limits on the field of view and the angular location of the target may also be specified by field angles  $\alpha_{uh}$ ,  $\alpha_{lh}$ , and  $\alpha_{th}$ , measured with respect to the horizon (a line perpendicular to the offset axis). Field angles above the horizon are considered positive while those below the horizon are negative; for the PAL system shown in Figure 2,  $\alpha_{uh} = 47^\circ$  and  $\alpha_{lh} = 12^\circ$ .

Quantitative analysis of moiré fringe patterns contained in a PAL image requires an accurate knowledge of the mapping function used to form the annular image. This function can be established empirically by placing the lens within a pipe of known radius. The optical axis of the PAL is aligned with the longitudinal axis of the pipe and a grid, consisting of equally spaced lines, is wrapped around the pipe wall to form a set of circles spaced equally along  $z$ . The axial field angle for each grid line (target),  $\alpha_t$ , is calculated and the corresponding radial position,  $r'_t$ , is measured in the image plane with respect to the polar coordinate system shown in Figure 1b. The values for  $r'_t$  are divided by the outer radius of the image,  $r'_o$ , to obtain a dimensionless ratio. A quadratic least squares fit is applied to the data in the plot of  $\alpha_t$  versus  $r'_t/r'_o$  to establish the mapping function. Figure 6 shows the result of applying this procedure to the PAL system shown in Figure 2. In this case,

$$\frac{r'_t}{r'_o} = 0.0911 \alpha_t^2 + 0.5639 \alpha_t + 0.0634 \quad (1)$$

In summary, the mapping between real space and image space is established empirically, and the mapping function relates distances to target points in the image plane to their corresponding axial field angles measured from the offset axis of the lens. As shown in Figure 7, each axial field angle may be associated with the distance measured from the offset point to the target point and linear dimensions measured in the  $z$  direction along the inside wall of the pipe. In the figure,  $r_p$  denotes the radius of the pipe;  $r_o$  is the radial offset. The distances  $l_u$ ,  $l_l$ , and  $l_t$  are associated with the upper, lower, and target axial field angles;  $d_t$  is the distance from the lowest point imaged by the lens to the target.

As illustrated in the following section, these definitions and parameters may be used to develop analytical relationships to predict or analyze moiré fringes produced by double exposure of gratings fixed to a cavity wall.



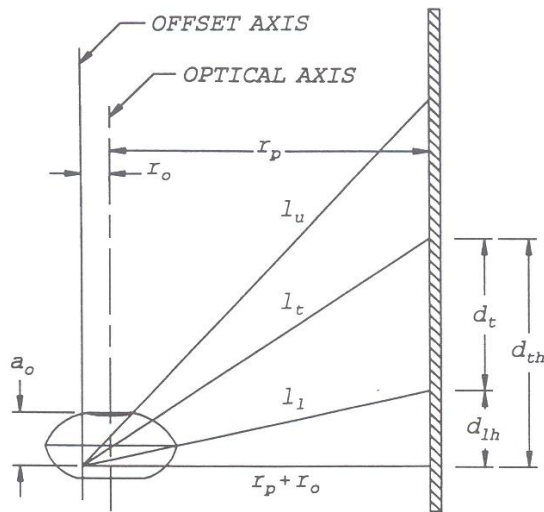


**Figure 7.** Field angles are associated with the distance measured from the offset point to the target point and linear dimensions measured along the cavity wall.

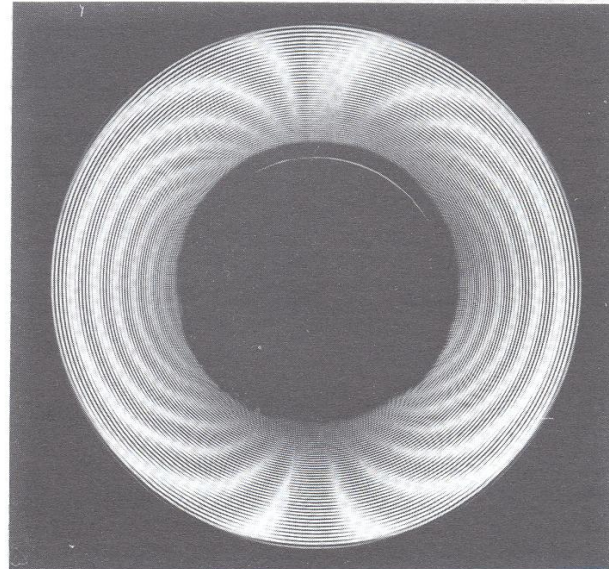


**Figure 8.** Moiré pattern recorded using a 50 mm diameter PAL. Fringes were produced by double exposure and correspond to the translation of a pipe section through 10.16 mm (0.4") along the x axis.

## 6. EXPERIMENTAL

Referring to the coordinate axes in Figure 4, the PAL system shown in Figure 3 was positioned within a 14 cm (5.5") diameter pipe so that the optical axis of the lens and the longitudinal axis of the pipe coincided with the z-direction. A grating of constant pitch equal to 1.27 mm (0.05") was wrapped around and attached to the interior wall of the pipe, creating a set of equally spaced rings parallel to the xy plane. These rings are mapped by the lens to the image plane as concentric circles, spaced at different distances apart. When the pipe was translated along the x direction through a displacement equal to 10.16 mm (0.4"), the nonlinear circular grating formed in the image plane distorted. Figure 8 shows the moiré pattern created by superimposing images recorded before and after the pipe was translated.

There are several ways in which these moiré fringes can be analyzed but for this application it is convenient to base the analysis on geometry. The two gratings have a line width to space ratio of one. When they are superimposed, moiré interference fringes are produced; low contrast occurs in areas where the dark lines of one grating fall into the spaces of the other, whereas high contrast is observed when the dark lines of one grating coincide with the other.

The loci of the fringes in Figure 8 can be predicted by considering Figure 7 which shows a section of the pipe wall viewed through the PAL. The distance from the horizon to the target is given by,

$$d_{th} = l_t \sin \alpha_{th} \quad (2)$$

where  $l_t$  is the distance measured from the offset point to the target point and  $\alpha_{th}$  is the field angle measured with respect to the horizon.

The perpendicular distance from the offset axis to the wall of the pipe is given by,

$$(r_p + r_o) = l_t \cos \alpha_{th} \quad (3)$$

Dividing Equation (2) by Equation (3) and using  $\alpha_{th} = (90 - \alpha_p)$ ,

$$\frac{d_{th}}{(r_p + r_o)} = \tan \alpha_{th} = \tan (90 - \alpha_p) \quad (4)$$

where  $\alpha_p$  is the axial field angle measured to the target point.

Solving for  $d_{th}$ ,

$$d_{th} = (r_p + r_o) \tan (90 - \alpha_p) \quad (5)$$

A similar argument can be applied to determine  $d_{lh}$ , the distance from the horizon to the point imaged at the lower field angle. That is,

$$d_{lh} = l_i \sin \alpha_{lh} \quad (6)$$

$$(r_p + r_o) = l_i \cos \alpha_{lh} \quad (7)$$

$$\frac{d_{lh}}{(r_p + r_o)} = \tan \alpha_{lh} = \tan (90 - \alpha_p) \quad (8)$$

$$d_{lh} = (r_p + r_o) \tan (90 - \alpha_p) \quad (9)$$

The distance from the target to the point imaged at the lower field angle is found by subtracting Equation (9) from Equation (5). That is,

$$d_t = d_{th} - d_{lh} = (r_p + r_o) [\tan(90 - \alpha_p) - \tan(90 - \alpha_p)] \quad (10)$$

Introducing the trigonometric identity,  $\cot \alpha_i = \tan (90 - \alpha_i)$ ,

$$d_t = (r_p + r_o) (\cot \alpha_i - \cot \alpha_p) \quad (11)$$

In predicting the fringe loci,  $d_t$  will be treated as the independent variable, and  $\alpha_i$  will be treated as the dependent variable. The axial field angle measured from the offset axis to the point under investigation can be determined from Equation (11) as,

$$\alpha_i = \tan^{-1} \left( \frac{1}{\frac{d_t}{(r_p + r_o)} + \frac{1}{\tan(\alpha_p)}} \right) \quad (12)$$

In Equation (12),  $\alpha_i$  is the lower axial field angle,  $d_t$  is the distance from the lowest point which can be seen through the PAL to the point under investigation,  $r_p$  is the radius of the pipe in which the PAL is inserted, and  $r_o$  is the radial offset of the lens.

Equations (1) and (12) can be combined to predict the locations of grating lines before and after displacement. A program was written to pinpoint the centers of bright lines in the image plane for the undisplaced case, and the center of dark lines in the displaced case. When a bright center from the undisplaced case coincides with a dark center from the displaced case, a half order fringe results. The fringe pattern shown in Figure 9 is obtained when these

calculations are made for a series of angles around the circumference of the image. This fringe pattern is in good agreement with that shown in Figure 8.

## 7. DISCUSSION

The moire pattern shown in Figure 8 is fairly complex considering that it corresponds to a simple translation. Contrary to analysis of conventional moire patterns which are governed by relatively simple equations, the analysis of panoramic moire patterns involves a mapping function and a detailed knowledge of the optical properties of the PAL imaging system.

Future research will address more complex cases in which the cavity wall rotates and deforms. It is hoped that qualitative evaluation will be aided by linearizing the PAL images.<sup>7</sup> Quantitative analysis should be enhanced by the development of field equations for panoramic moire.

## 8. CONCLUSIONS

Panoramic moire is a new technique for radial metrology which relies on a unique panoramic annular lens (PAL) to capture a flat annular image of the entire 360 degree surround of its optical axis. Definitions and parameters required for the analysis of panoramic moire patterns were introduced along with a procedure for establishing a suitable mapping function for the lens. Experimental results verified analytical arguments.

The most outstanding attributes of the panoramic measurement system are that there are no moving parts, the surrounding area can be viewed simultaneously, and the depth of focus is infinite. Despite the relatively complex analysis required for panoramic moire, the technique may ultimately address many of the requirements for measurement associated with aerospace hardware and space-based systems.

## 9. ACKNOWLEDGEMENTS

PAL research is supported by Optechnology, Inc, and has been funded by NASA's Marshall Space Flight Center under Contract Nos. NAG8-686, NAG-159, and NAS8-36955 Delivery Order 124. The authors would like to acknowledge the interest and support of several personnel at the Marshall Space Flight Center including Jack Lee, Director; Bill Lucas, former Director; James Moses of the Research and Technology Office; Ann Whitaker, Ken Woodis, and Ron Beshears of the Materials and Processes Laboratory; John McCarty, Eric Hyde, Gary Lyles, and Jay Nichols of the Propulsion Laboratory; and, Jonathan Campbell of the Space Sciences Laboratory who first entertained our proposal to "Change The World's Perspective."

## 10. REFERENCES

1. Durelli, A.J., Parks, V.J., Moire Analysis of Strain, Prentice-Hall Inc., Englewood Cliffs, N.J., 1970.
2. Greguss, P., U.S. Patent No. 4,566,763, 1984.
3. Matthys, D.R., Greguss, P., Gilbert, J.A., Lehner, D.L., Kransteuber, A.S., "Radial metrology with a panoramic annular lens," Proc. of SPIE's 33rd. Annual International Symposium on Optical & Optoelectronic Applied Science & Engineering, San Diego, California, August 6-11, 1989.
4. Gilbert, J.A., Matthys, D.R., Greguss, P., "Optical measurements through panoramic imaging systems," Proc. of the 1990 Int. Conf. on Hologram Interferometry & Speckle Metrology, Baltimore, Maryland, November 4-7, 1990, pp. 164-171.
5. Gilbert, J.A., Matthys, D.R., Lehner, D.L., Hendren, C.M., "Panoramic imaging systems for nondestructive

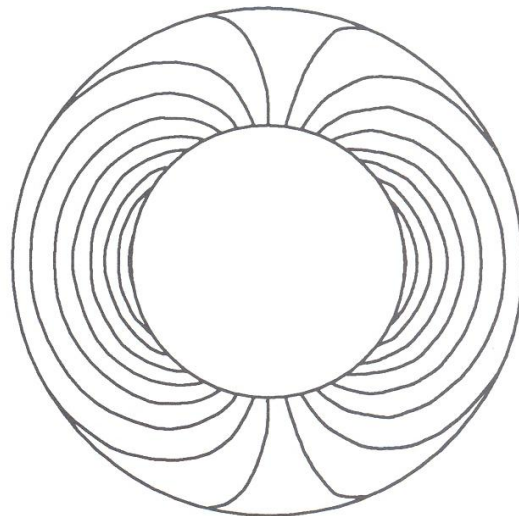


**Figure 9.** Fringe loci for the moire pattern shown in Figure 8 obtained from theory.



- evaluation," Proc. of the Third Conference on Nondestructive Evaluation for Aerospace Requirements, Huntsville, Alabama, June 4-6, 1991.
6. Bankston, C.D., Gilbert, J.A., "Tethers and their role in the space exploration initiative," under consideration for presentation and publication in Proc. of the ASCE Third International Conference on Engineering, Construction and Operations in Space, Denver, CO, May 31 - June 4, 1992.
  7. Matthys, D.R., Gilbert, J.A., Puliparambil, J., "Endoscopic inspection using a panoramic annular lens," Proc. of SPIE's 1991 International Symposium on Optical & Optoelectronic Applied Science & Engineering, San Diego, California, July 21-26, 1991.